Valence-band structure of the polar ZnO surfaces studied by angle-resolved photoelectron spectroscopy

K. Ozawa,[1,*] Y. Oba,[2] K. Edamoto,[2] M. Higashiguchi,[3] Y. Miura,[3] K. Tanaka,[3] K. Shimada,[4] H. Namatame,[4] and M. Taniguchi[3,4]

[1]*Department of Chemistry and Materials Science, Tokyo Institute of Technology, Ookayama, Meguro-ku, Tokyo 152-8551, Japan*

[2]*Department of Chemistry, Rikkyo University, Nishi-Ikebukuro, Toshima-ku, Tokyo 171-8501, Japan*

[3]*Graduate School of Science, Hiroshima University, Higashi-Hiroshima 739-8526, Japan*

[4]*Hiroshima Synchrotron Radiation Center, Hiroshima University, Higashi-Hiroshima 739-0046, Japan*

(Received 11 September 2008; revised manuscript received 21 December 2008; published 12 February 2009)

Valence-band structures of the polar ZnO surfaces, i.e., ZnO(0001)-Zn and ZnO($000\bar{1}$)-O, have been investigated by angle-resolved photoelectron spectroscopy utilizing synchrotron radiation. On the (1×1) O-terminated surface, surface-localized states forming dispersing bands with a (1×1) periodicity are identified at the upper portion of the valence-band region. The energetic position of these states and the fact that their photoemission intensities are sensitive to gas adsorption suggest that there is a contribution from the O $2p$ dangling-bond orbital of the surface O atoms. Comparing the valence-band structure of the ($000\bar{1}$)-O surface with that of the (0001)-Zn surface, a deviation of the electronic structure in the near surface region from that in the bulk is found to be larger on (0001)-Zn than on ($000\bar{1}$)-O. The role of the step structures, which exist on both polar surfaces but with much higher density on the (0001)-Zn surface, in the modification of the electronic structure is discussed.

DOI: 10.1103/PhysRevB.79.075314 PACS number(s): 73.20.−r, 79.60.−i

I. INTRODUCTION

Understanding the stabilization mechanism of polar ZnO surfaces has long been one of the challenging problems in surface science. Low-energy electron diffraction (LEED) measurements have revealed that both Zn-terminated (0001) surface (ZnO-Zn) and O-terminated ($000\bar{1}$) surface (ZnO-O) exhibit (1×1) patterns,[1–3] suggesting that these polar surfaces are bulk terminated. Photoelectron diffraction study,[4] ion scattering spectroscopy (ISS) study,[5] and surface x-ray diffraction (XRD) study[6,7] have all suggested the (1×1) bulk-terminated structures of the polar ZnO surfaces. The bulk-terminated polar surfaces are, in principle, unstable because of nonvanishing dipole moment perpendicular to the surface.[8,9] Therefore, there should exist some stabilization mechanisms to maintain the long-range (1×1) structures of the polar ZnO surfaces.

Scanning tunneling microscopy (STM) studies for the (1×1) ZnO-Zn surface[2,10,11] have revealed that triangular-shaped pits and islands are formed on the (1×1) terraces, and as a result the ZnO-Zn surface becomes highly stepped. Dulub *et al.*[10] proposed from the STM study combined with *ab initio* calculations that formation of the pits and islands is essential to stabilize the ZnO-Zn surface, since the step edges of these microstructures are O terminated so that the concentration of the surface Zn atoms is decreased to balance the surface charge density.

The ZnO-O surface, on the other hand, must be stabilized by a different mechanism from that on the ZnO-Zn surface because surface morphology of ZnO-O is characterized by smooth terraces with a considerably low step density.[2] *Ab initio* slab calculations carried out so far have predicted a strong contraction of the outermost O-Zn double-layer spacing by roughly 40%–50% of the bulk value on the O-terminated surface.[7,9,12] The contraction of the double-layer spacing has also been deduced experimentally by several groups using the XRD technique.[6,7] Thus, surface relaxation may play some role to stabilize the ZnO-O surface. Contrary to the results of XRD, Overbury *et al.*[5] concluded from the ISS measurements that the double-layer spacing is nearly identical to the bulk value. Meyer and Marx[9] suggested that the absence of the double-layer contraction may be due to hydrogen adsorbing on the ZnO-O surface. A possible role of H adsorption on the ZnO-O surface has recently been proposed by Kunat *et al.*[13] They have concluded on the basis of their He-atom scattering experiments that the commonly obtained (1×1) ZnO-O surfaces are actually covered with a saturation amount of H atoms and that the H-free clean surface should undergo a (1×3) reconstruction.[13] However, Lindsay *et al.*[3] indicated that an almost H-free (1×1) surface can be obtained by conventionally employed cleaning procedure of sputtering-annealing cycles. Therefore, the stabilization mechanism of the (1×1) ZnO-O surface including the role of H remains an open question.

In order to elucidate the stabilization mechanism of the ZnO-O surface experimentally, it is necessary to determine the electronic band structures of the ZnO-O surface and to clarify whether the (1×1) structure results from H adsorption or not. Another important point to be clarified is how the electronic structures of the ZnO-O and ZnO-Zn surfaces are affected by surface termination; these polar surfaces have different atomic composition and different surface morphology with the same bulk structure. Thus far, only limited information is available on the electronic structure of the polar ZnO surfaces. Göpel *et al.*[14] first conducted angle-resolved photoelectron spectroscopy (ARPES) measurements to characterize the electronic structures of the polar ZnO surfaces. They found emission from the O $2p$ dangling-bond state at the upper part of the valence-band region on the ZnO-O surface, whereas emission from the Zn $4s$-O $2p$ back bond state

forms a peak at the middle of the valence band on ZnO-Zn. More recently, Girard *et al.*[15] performed detailed ARPES measurements and determined the two-dimensional band structure of the ZnO-Zn surface. The surface-localized bands with a (1×1) dispersion are identified at 4–5 and 7–8 eV below the Fermi level, and the authors have attributed these surface-localized states to the O $2p$-Zn $4p/3d$ and O $2p$-Zn $4s$ backbond states, respectively.[15]

Details of the valence-band structure of the ZnO-O surface, especially the band structure of the O $2p$-dangling-bond state, have not been clarified so far. In the present study, therefore, we have carried out ARPES measurements to determine the electronic structure of the (1×1) ZnO-O surface. It is found that H_2O as a residual gas in the ultrahigh vacuum (UHV) chamber can adsorb on the ZnO-O surface at room temperature. This implies that the (1×1) ZnO-O surface obtained in the present study should not be saturated with H. We have identified several surface-localized states at the upper portion of the valence-band region. These states form bands with a substantial dispersion along the high-symmetry axes of the surface Brillouin zone (SBZ) with a (1×1) periodicity. We have also carried out ARPES measurements of the ZnO-Zn surface and compared the band structure to that of ZnO-O in order to elucidate the effect of the surface termination on the electronic structure. The dispersion relation of the bulk bands is found to depend on morphology of these two surfaces. Cu deposition experiment clearly indicates that the electronic structure in the near-surface region of the ZnO-Zn surface is significantly modified in comparison to that of the ZnO-O surface.

II. EXPERIMENT

The ARPES measurements were made at liner undulator beamline (BL-1) of a compact electron-storage ring (HiSOR) at Hiroshima University.[16] A Scienta SES200 electron-energy analyzer was used to obtain the photoemission spectra. The angular resolution of the photoelectrons was set to 0.4° and total-energy resolution was estimated to be 37 meV at the photon energy ($h\nu$) of 50 eV. The base pressure of the UHV chamber was lower than 2×10^{-8} Pa.

A both-side polished ZnO crystal with the (0001) orientation ($10\times10\times0.5$ mm^3) was purchased from Goodwill Co. The crystal was divided into three pieces and two pieces were used for the measurements: one for the Zn-terminated surface and the other for the O-terminated surface. The remaining piece was used to distinguish the surface termination by examining the etching behavior of both sides of the crystal plate in 1 M HCl solution for 5 min; the O-terminated surface is etched more easily than the Zn-terminated surface.[17] The ZnO samples were fixed on Mo sample holders and mounted on a multiaxis goniometer (*i*-Gonio LT, R-Dec Co.),[18] which enabled us to precisely change polar, azimuth, and tilt angles of the sample. The ZnO-O and ZnO-Zn surfaces were cleaned by cycles of Ar^+ sputtering (2 kV, ~1 μA) and annealing at 1050–1100 K in UHV. The clean surfaces of ZnO-O and ZnO-Zn thus prepared showed sharp (1×1) LEED patterns.

The Cu deposition experiment was carried out at BL 1C of the Photon Factory, High Energy Accelerator Research Organization. The UHV chamber was equipped with a hemispherical electron energy analyzer (VSW HA45) with a microchannel-plate electron multiplier for the ARPES measurements. The angular resolution was $\pm1°$ and the energy resolution was 130 meV at $h\nu=50$ eV. The base pressure of the system was $\sim2\times10^{-8}$ Pa. Cu was vapor deposited onto the surfaces at room temperature from the evaporation source (Omicron EFM3). Cu was evaporated from a high-purity Cu rod (99.995%) by electron bombardment. The Cu coverage was estimated from the intensity of the Zn $3p$ core-level peak, which we assume decays exponentially as a function of the average thickness of the Cu overlayer. One monolayer (ML) corresponds to the coverage where the Cu overlayer with the average thickness of 0.256 nm is formed.

All ARPES spectra presented in this paper were acquired at room temperature. The electron binding energy is referenced to the Fermi level, which was determined from the Fermi cutoff in the spectra of Mo sample holders.

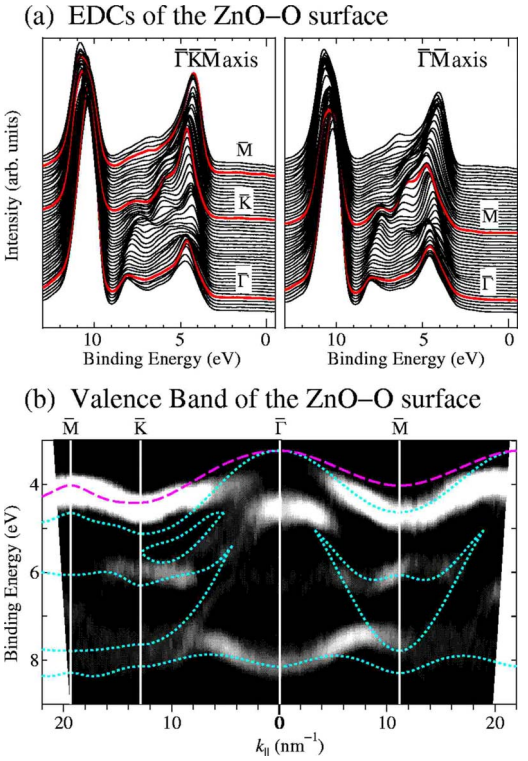

FIG. 1. (Color online) (a) EDCs of the ZnO-O surface along the $\overline{\Gamma M}$ and $\overline{\Gamma KM}$ axes. The incident photon energy was 50 eV. (b) The intensity plot of the second derivatives of the measured EDCs. Bright and dark regions correspond to the high and low spectral weight regions, respectively. Dotted lines indicate the edges of the PBB, which is obtained from the empirical TB calculations (Ref. 19). Dashed line shows the upper edges of the PBB given by the DFT calculations (Ref. 20).

III. RESULTS AND DISCUSSION

A. Surface electronic structure of ZnO-O

Figure 1(a) shows energy distribution curves (EDCs) of the O-terminated surface along the high-symmetry axes of

the SBZ ($\overline{\Gamma KM}$ and $\overline{\Gamma M}$). The valence spectra of ZnO are roughly divided into two parts: one in the binding-energy region between 3 and 9 eV is composed of emission from the O $2p$-Zn $4sp$ hybridized states and the other with a sharp peak at 10.7 eV corresponds to the Zn $3d$ band. The O $2p$-Zn $4sp$ states form several bands with dispersing features. To visualize the dispersion relation between the binding energy of the O $2p$-Zn $4sp$ states and the surface parallel component of the wave-number vector $k_{\|}$, a grayscale band map is constructed by plotting spectral weights of the second derivatives of the measured EDCs [Fig. 1(b)]. The O $2p$-Zn $4sp$ bands are seen as bright regions. Three bands are observed at 4–5 eV with a strong emission intensity: one at around the center of the SBZ ($\bar{\Gamma}$) and the other two at around the zone boundaries ($\bar{K}$ and $\bar{M}$). Two branches with a weaker intensity are seen at ~6 eV in the vicinities of $\bar{K}$ and $\bar{M}$. Also observed is a band with a clear dispersion at ~8 eV.

Dotted lines in Fig. 1(b) indicate the edges of the projected bulk-band (PBB) region, which were obtained by empirical tight-binding (TB) calculations by Ivanov and Pollmann.[19] A dashed line is the upper edge of the PBB region given by density-functional theory (DFT) calculations by Kresse *et al.*[20] The energetic positions of these theoretical lines are adjusted so that the valence-band maximum at $\bar{\Gamma}$ coincides with the leading edge of the measured normal-emission spectra (3.2 eV). It is clear that the upper-edge structure of the PBB depends strongly on the calculation methods; although the dispersion behavior of the upper edge is similar in both results, the dispersional band width given by the TB calculations appears to be larger than that given by the DFT calculations. If we compare the experimental bands to the result by the TB calculations, the O $2p$-Zn $4sp$ band at 4–5 eV along the $\overline{\Gamma KM}$ axis exists within the band gap above the upper edge. On the other hand, all valence bands lay below the upper edge of the PBB by the DFT calculations. Therefore, it cannot be determined whether the band exists within the band gap by simply comparing the experimental result to the theoretical band structures. As we will show below, however, no state exists in the band gap above the upper edge of the PBB. The shallowest-lying bands at ~4 eV are still observed even after the ZnO-O surface is covered with foreign molecules that quench emission from the surface-localized states.

On the ideally terminated ZnO-O surface, the O $2p$ dangling-bond states should exist since the surface is terminated by the coordinatively unsaturated O atoms. These dangling-bond states are sensitive to adsorption of foreign species on the surface. Thus, in order to identify the expected surface-localized states on the (1×1) ZnO-O surface, we have measured the ARPES spectra of the clean and contaminated surfaces and compared the EDCs. In Figs. 2(a) and 2(b), we show the ARPES spectra of the ZnO-O surface measured within 3 h after the sample cleaning, namely, the clean surface, and those measured more than 12 h later to allow residual gasses in the chamber to be adsorbed on the surface, namely, the contaminated surface. The EDCs of the clean and contaminated surfaces are normalized to the intensity at the binding energies between 13 and 14 eV. Suppression of the emission intensity is observed in the energy region between 4 and 6 eV, while the intensity in the deeper region (6–8 eV) is not much affected for most of the EDCs. In order to resolve the surface-localized states, we took differences between the EDCs of the clean surface and those of the contaminated surface. An example of the difference EDCs is shown in Fig. 2(c). Peak structures, indicated by arrows, are associated with the adsorption-sensitive and thus surface-localized states. These states form dispersing bands along the $\overline{\Gamma KM}$ and $\overline{\Gamma M}$ axes as depicted by bright bands in Fig. 3, which shows intensity plots of the difference EDCs. The surface-localized states form several dispersing bands between 4 and 5 eV; one is observed at around the center of the SBZ with an binding-energy minimum at $\bar{\Gamma}$ and the other two bands have binding-energy maxima at the zone boundaries ($\bar{K}$ and $\bar{M}$). A flat band is also seen at ~6 eV at around

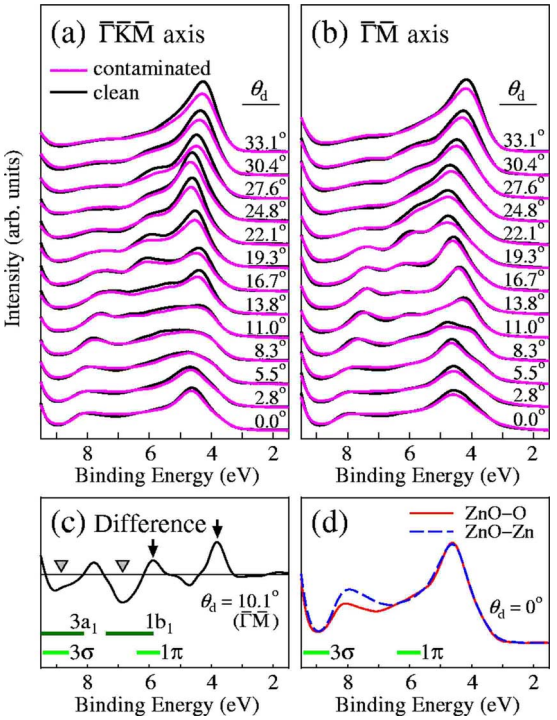

FIG. 2. (Color online) EDCs of the clean and contaminated ZnO-O surfaces ($h\nu$=50 eV) along (a) $\overline{\Gamma KM}$ and (b) $\overline{\Gamma M}$. The detection angles θ_d are measured from the surface-normal direction. The EDSs of the contaminated surface are shifted by 0.15 eV toward the lower-binding-energy side to compensate adsorption-induced downward band bending. (c) An example of the difference spectra between the EDCs of the contaminated surface and those of the clean surface (θ_d=10.1° on the $\overline{\Gamma M}$ axis). Arrows indicate the surface-localized adsorption-sensitive peaks. Dip structures, pointed by triangle marks, correspond to the emissions from the molecular orbitals of adsorbed species. (d) Normal-emission spectra of the clean ZnO-O and ZnO-Zn surfaces ($h\nu$=50 eV). The ZnO-Zn spectrum is shifted by 0.3 eV toward the lower-binding-energy side to compensate the difference in band bending on both surfaces. Horizontal bars in Figs. 2(c) and 2(d) indicate the positions where the emission peaks from the molecular orbitals of H_2O ($1b_1$ and $3a_1$) and OH (1π and 3σ) are observed in the photoemission spectra reported in Refs. 23 and 24.

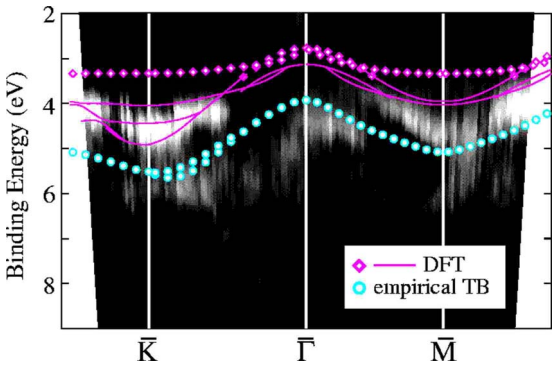

FIG. 3. (Color online) (a) The intensity plot of the difference spectra between the spectra of the clean surface and those of the contaminated surface shown in Fig. 2. Bright areas correspond to the surface-localized bands. Lines indicated by open symbols are the theoretically derived surface-localized O $2p$ dangling-bond bands by the empirical TB study (Ref. 19) and by the DFT study (Ref. 20). The bands localized at the second and third O-Zn double layers, given by the DFT calculations, are also shown by solid lines.

$\bar{K}$. Overall dispersive features of the surface-localized states are consistent with the (1×1) periodicity.

Before moving on to the discussion of the origin of the surface-localized bands, we should characterize the atomic composition of the (1×1) ZnO-O surface prepared in the present study. Kunat *et al.*[13] proposed that the (1×1) surfaces commonly reported in the literatures should be saturated with H atoms and that the clean surface has a (1×3) structure. On the other hand, Lindsay *et al.*[3] indicated that the H-free (1×1) surface can be realized. In the present study, the (1×1) ZnO-O surface is found to allow foreign molecules to be adsorbed at room temperature. A slight enhancement of the emission intensity is seen at ~7 and 9 eV in some of the EDCs of the contaminated surface [Figs. 2(a) and 2(b)], and such enhancements are depicted as dip structures in the difference spectrum [Fig. 2(c)]. Similar adsorption-induced structures are also observed when H_2O adsorbs on the ZnO surfaces,[21,22] and they have been associated with the molecular orbitals of adsorbed H_2O ($1b_1$ and $3a_1$) (Ref. 23) and/or OH (1π and 3σ).[24] Thus, adsorbed species are most probably H_2O, which is one of molecules with the highest sticking probability among the residual gasses in the UHV chamber. If the (1×1) ZnO-O surface is saturated with H, H_2O cannot be adsorbed on such a surface in an UHV condition at room temperature because of a very low sticking probability.[25] Therefore, it is reasonable to consider that, though a small amount of H may exist on the surface, the (1×1) ZnO-O surface prepared in the present study is a H-free surface.

In order further to support our conclusion that the ZnO-O surface is not saturated with H, we compared the spectrum of the clean ZnO-O surface to that of the clean ZnO-Zn surface, on which the amount of adsorbed OH as a contaminant is considered to be small.[2,11] Figure 2(d) shows the normal-emission spectra of the ZnO-O and ZnO-Zn surfaces. Both spectra are normalized to the intensity at 13–14 eV. The ZnO-Zn spectrum is shifted by 0.3 eV toward the lower-binding-energy side to compensate the difference in band binding on both surfaces. It is apparent that the emission intensities of the ZnO-O spectrum at ~6 and 9 eV, where the OH 1π and 3σ peaks are expected,[24] are neither enhanced nor suppressed in comparison to the ZnO-Zn spectrum. Although such a comparison is not decisive, we speculate that the clean ZnO-O surface obtained by our preparation procedure should not be covered with a saturation amount of H.

The ARPES measurements reveal that the surface-localized bands exist in the upper part of the ZnO valence-band region on the H-free ZnO-O surface. Theoretical studies have also yielded the O $2p$ dangling-bond bands in the upper portion of the valence-band region on the H-free (1×1) ZnO-O surface.[7,12,19,20] Thus, the experimentally identified surface-localized bands can be associated with the O $2p$ dangling-bond bands. In Fig. 3, we compare the experimental band structure to theoretically derived surface-localized O $2p$ dangling-bond bands (lines indicated by open symbols) given by the empirical TB (Ref. 19) and DFT (Ref. 20) studies. Also shown by solid lines are the DFT bands, which are localized at the second and third O-Zn double layers.[20] The energetic positions of the theoretical bands are adjusted so that the valence-band maximum of the PBB coincides with 3.2 eV. The O $2p$-dangling-bond bands by both theoretical studies qualitatively reproduce the experimental bands in that the bands have a binding-energy minimum at $\bar{\Gamma}$ and disperse toward the higher binding energies to reach the binding-energy maxima at $\bar{K}$ and $\bar{M}$. If the bands by the TB calculations are shifted upwards by ~1 eV, they overlap satisfactorily with the experimental bands at 4–5 eV at around the zone boundaries ($\bar{K}$ and $\bar{M}$). On the other hand, because of the small dispersion width of the DFT bands shown by the open diamonds, the agreement between the theory and the experiment is rather poor even if the bands are vertically shifted. It is noted that the bands drawn by the solid lines seem to explain the experimental bands at around the zone boundaries (especially at around the $\bar{K}$ point) without energy adjustment. However, these bands are localized between the third layer and the sixth layer (counted from the surface).[20] Since the experimentally derived bands should be strongly localized at the outermost surface layers, we consider that such an agreement should be coincidental. Obviously, further theoretical studies are needed to comprehensively describe the surface electronic structure of the H-free (1×1) O-terminated surface.

Regarding the stabilization mechanism of the H-free ZnO-O surface, all theoretical studies by the DFT slab calculations have predicted that the ZnO-O surface is stabilized by reducing surface negative charge and by forming a partially filled O $2p$ dangling-bond bands.[7,12,20] However, no band crossing the Fermi level is observed in the present study and this is in good agreement with an earlier experimental study.[26] This indicates that the H-free (1×1) ZnO-O surface is stabilized not by a simple charge balance. We assume that the band structure of the O $2p$ dangling-bond states identified in the present study is helpful for theoretical efforts to understand the stabilization mechanism.

B. Effect of surface polarity on the electronic structure

In Sec. III A, we have presented the valence-band structure of the (1×1) ZnO-O surface. Although a contribution

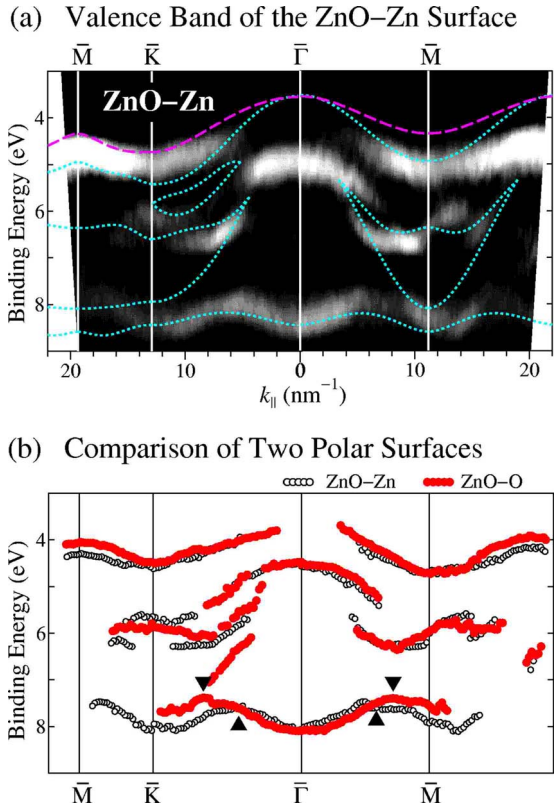

FIG. 4. (Color online) (a) The intensity plot of the second derivatives of the ARPES spectra of the ZnO-Zn surface. Dotted and dashed lines are the same as shown in Fig. 1(a). The valence-band maximum at $\bar{\Gamma}$ is determined to be 3.5 eV so that the binding energy of the upper edges of the PBB is adjusted to 3.5 eV. (b) Comparison of the band structures of ZnO-O and ZnO-Zn. Only the branches with a strong intensity are plotted. The bands of the ZnO-Zn surface are offset by 0.3 eV. Triangle marks indicate the position of the binding-energy minima of the bands.

from the surface-localized bands is identified in the upper portion of the valence-band region, the observed bands are mostly attributed to the bulk bands projected onto the $\bar{\Gamma}\bar{K}\bar{M}$ and $\bar{\Gamma}\bar{M}$ axes since the emission intensity from the surface-localized bands is much weaker than the bulk-band emission (Fig. 2).

Figure 4(a) shows the intensity plot of the second derivatives of the ARPES spectra of the ZnO-Zn surface. The measurement condition was the same as the ZnO-O surface. Although the valence-band structure of ZnO-Zn obtained in the present study is more complex than that reported earlier by Girard *et al.*,[15] the overall features in both studies are similar to each other. Surface-localized states have also been identified on ZnO-Zn and assigned to the Zn-O backbond states in the earlier studies.[14,15] However, a contribution of these states to the observed photoemission intensity is expected to be small especially at the upper portion of the valence-band region.[14] Thus, as in the case of the ZnO-O surface, the ZnO-Zn bands shown in Fig. 4(a) are mostly composed of emission from the bulk bands.

The valence-band structure of the ZnO-Zn surface is, at first glance, similar to that of the ZnO-O surface [Fig. 1(b)]. This is reasonable because the measured bands of both surfaces have a large bulk contribution. In Fig. 4(b), we compare the band structures of both polar surfaces. The bands of the ZnO-Zn surface are shifted by 0.3 eV toward the lower-binding-energy side to compensate the difference in band bending of both surfaces. There are two notable differences in the band structure: (i) the bands at the top of the valence-band region (4–4.5 eV) have a different dispersion width along $\bar{K}\bar{M}$ and $\bar{M}\bar{\Gamma}$; (ii) the bottom bands at ~8 eV show different dispersion structure; namely, the binding-energy minima of the bands, indicated by triangle marks, appear at different $k_{\|}$ positions. Considering that the observed bands are bulk derived, such a surface dependence seems peculiar.

We consider that the surface dependence of the bulk bands should be a consequence of different morphologies of the polar ZnO surfaces. The STM studies have revealed that the ZnO-Zn surface is characterized by a number of step structures with a double-layer step height (0.26 nm).[2,10,11] On the other hand, the ZnO-O surface has wide and smooth terraces with a low step density.[2] At these step edges, a dipole moment with a surface-parallel component should be induced. An electrostatic field induced by the step-induced dipole must be canceled out when the whole surface area is considered. Thus, the electronic structure deep inside the bulk is insensitive to the difference of surface morphology. However, a significant influence from the step structure is expected for the electronic structure in the near-surface region. In the present ARPES study, the detected photoelectrons come from the several atomic layers in the surface region, since the inelastic mean-free path of the photoelectrons with the kinetic energy of 38–44 eV, which corresponds to the valence-band region, is 0.3–0.37 nm.[27] It is, therefore, plausible that we observe the electronic structure which is under a strong influence of the surface condition and that the different bulk-band structures of two polar ZnO surfaces originate from the different step densities on these surfaces.

In order to confirm the above-mentioned hypothesis, we have investigated the electronic structures of the Cu-covered polar ZnO surfaces and compared them to those of the clean surfaces. It is found that deposition of Cu induces emission from the Cu 3*d* states between 2 and 6 eV. Thus, the band at the bottom of the valence region (~8 eV) can be followed without the interference of Cu 3*d* emission. The upper panel of Fig. 5(a) shows the deepest-lying band of the clean ZnO-Zn surface. Triangle marks with error bars indicate the positions of binding-energy maxima and minima of the band. When the ZnO-Zn surface is covered with Cu (the coverage is ~5 ML), the maxima and minima of the band shift to larger $k_{\|}$ [the lower panel of Fig. 5(a)]. For example, the binding-energy minima at 8.4 nm^{-1} on $\bar{\Gamma}\bar{K}$ and 7.2 nm^{-1} on $\bar{\Gamma}\bar{M}$ are shifted, respectively, to 9.4 and 8.3 nm^{-1} upon Cu adsorption. On the other hand, Cu adsorption hardly affects the positions of a maximum and minima of the bands on the ZnO-O surface [Fig. 5(b)]. The positions of the binding-energy minima on $\bar{\Gamma}\bar{K}$ are 9.6 and 9.7 nm^{-1} on the clean and 3.5-ML Cu-covered surfaces, respectively. Interestingly, these values are almost the same as the corresponding binding-energy minimum of the band on the Cu/ZnO-Zn surface (9.4 nm^{-1}). From these observations, we assume that the bands on the Cu/ZnO-Zn surface and on the clean and

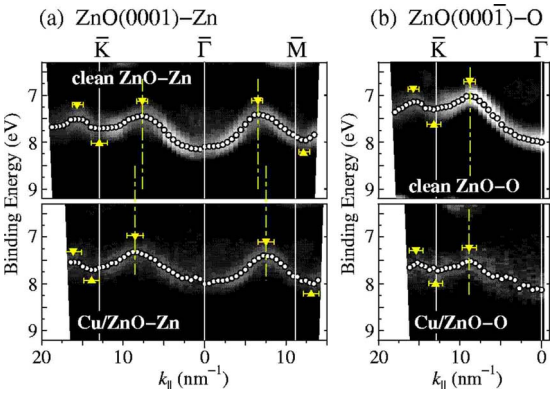

FIG. 5. (Color online) (a) The intensity plot of the second derivatives of the ARPES spectra from the clean (upper) and the Cu-covered (lower) ZnO-Zn surfaces. The states at the bottom of the valence-band region are shown as bright bands. Open circles indicate the peak positions in the second derivatives. Triangle marks with error bars indicate the positions of the binding-energy maxima and minima of the dispersing bands. Vertical dot-dash lines are placed to clarify the Cu-induced change in the binding-energy minimum positions. (b) The same as Fig. 5(a) but the results for the ZnO-O systems.

Cu-covered ZnO-O surfaces should have a more bulklike character than the band on the clean ZnO-Zn surface.

The STM studies have revealed that the deposited Cu atoms on the polar ZnO surfaces form clusters and a majority of these clusters occupy the sites on the terraces on both ZnO-Zn and ZnO-O surfaces at the initial stages of adsorption (below 1 ML).[28,29] However, Cu clusters at high Cu coverages are found to be large enough to cover the step edges.[29] In the present study, we have examined the polar ZnO surfaces covered with ~5-ML Cu, with which ~60% of the substrate surfaces are covered. Thus, it is safe to conclude that the step edges on the polar surfaces, though not all of them, are affected by Cu. The Cu atoms at the step sites must be polarized so as to cancel the step-induced dipole moment. Thus, the electrostatic field induced by the step dipoles should be reduced or completely quenched on the Cu-covered surfaces. Considering that the step density is higher on the ZnO-Zn surface than the ZnO-O surface, the effect of Cu adsorption is expected to be larger on the former surface than the latter. This is what we actually observe in the Cu-adsorption experiment; the ZnO valence band in the near-surface region on the ZnO-Zn surface is modified by Cu adsorption, whereas that on the ZnO-O surface is not. Therefore, we conclude that the electronic structures within the several atomic layers from the polar ZnO surfaces depend on the surface termination which is directly related to surface morphology.

IV. SUMMARY

In the present ARPES study, we have examined the electronic structure of the (1×1) ZnO(000$\bar{1}$)-O surface. The surface-localized states are identified at the upper part of the valence-band region and are assigned to the O $2p$ dangling-bond states. The two-dimensional structure of these states has also been examined and it is found that the states form bands with a (1×1) periodicity. No state is observed within the band-gap region of ZnO.

The difference in the electronic structures of the ZnO-O and ZnO-Zn surfaces is also examined and discussed. It is clarified that the dispersion structure of the bulk bands depends on the surface termination. Cu adsorption induces the structural change of the bands only on the ZnO-Zn surface, but not on the ZnO-O surface. This finding suggests that the electronic structure in the near-surface region of the ZnO-Zn surface is significantly influenced by surface morphology. Since the density of the step structure is higher on the ZnO-Zn surface than on the ZnO-O surface, the step-induced dipole moment significantly modifies the electronic structure of the ZnO-Zn surface, whereas such an effect is small on the ZnO-O surface.

ACKNOWLEDGMENTS

The synchrotron-radiation experiments were performed under the approvals of Hiroshima Synchrotron Radiation Center (HSRC) (Proposal No. 06-A-34) and the Photon Factory Advisory Committee (Proposal No. 2006G003). We thank the staff of HSRC and the Photon Factory for their excellent support.

*ozawa.k.ab@m.titech.ac.jp

[1] R. Leysen, B. J. Hopkins, and P. A. Taylor, J. Phys. C **8**, 907 (1975).
[2] O. Dulub, L. A. Boatner, and U. Diebold, Surf. Sci. **519**, 201 (2002).
[3] R. Lindsay, C. A. Muryn, E. Michelangeli, and G. Thornton, Surf. Sci. **565**, L283 (2004).
[4] M. Sambi, G. Granozzi, G. A. Rizzi, M. Casarin, and E. Tondello, Surf. Sci. **319**, 149 (1994).
[5] S. H. Overbury, P. V. Radulovic, S. Thevuthasan, G. S. Herman, M. A. Henderson, and C. H. F. Peden, Surf. Sci. **410**, 106 (1998).
[6] N. Jedrecy, M. Sauvage-Simkin, and R. Pinchaux, Appl. Surf. Sci. **162-163**, 69 (2000).
[7] A. Wander, F. Schedin, P. Steadman, A. Norris, R. McGrath, T. S. Turner, G. Thornton, and N. M. Harrison, Phys. Rev. Lett. **86**, 3811 (2001).
[8] C. Noguera, J. Phys.: Condens. Matter **12**, R367 (2000).
[9] B. Meyer and D. Marx, Phys. Rev. B **67**, 035403 (2003).
[10] O. Dulub, U. Diebold, and G. Kresse, Phys. Rev. Lett. **90**, 016102 (2003).
[11] F. Ostendorf, S. Torbrügge, and M. Reichling, Phys. Rev. B **77**, 041405(R) (2008).
[12] J. M. Carlsson, Comput. Mater. Sci. **22**, 24 (2001).

[13] M. Kunat, St. G. Girol, Th. Becker, U. Burghaus, and Ch. Wöll, Phys. Rev. B **66**, 081402(R) (2002).
[14] W. Göpel, J. Pollmann, I. Ivanov, and B. Reihl, Phys. Rev. B **26**, 3144 (1982).
[15] R. T. Girard, O. Tjernberg, G. Chiaia, S. Söderholm, U. O. Karlsson, C. Wigren, H. Nylén, and I. Lindau, Surf. Sci. **373**, 409 (1997).
[16] K. Shimada, M. Arita, Y. Takeda, H. Fujino, K. Kobayashi, T. Narimura, H. Namatame, and M. Taniguchi, Surf. Rev. Lett. **9**, 529 (2002).
[17] A. N. Mariano and R. E. Hanneman, J. Appl. Phys. **34**, 384 (1963).
[18] Y. Aiura, H. Bando, T. Miyamoto, A. Chiba, R. Kitagawa, S. Maruyama, and Y. Nishihara, Rev. Sci. Instrum. **74**, 3177 (2003).
[19] I. Ivanov and J. Pollmann, Phys. Rev. B **24**, 7275 (1981).
[20] G. Kresse, O. Dulub, and U. Diebold, Phys. Rev. B **68**, 245409 (2003).
[21] G. Zwicker and K. Jacobi, Surf. Sci. **131**, 179 (1983).
[22] K. Ozawa, Y. Oba, and K. Edamoto, Surf. Sci. **601**, 3125 (2007).
[23] M. A. Henderson, Surf. Sci. Rep. **46**, 1 (2002).
[24] P. A. Thiel and T. E. Madey, Surf. Sci. Rep. **7**, 211 (1987).
[25] M. Schiek, K. Al-Shamery, M. Kunat, F. Traeger, and Ch. Wöll, Phys. Chem. Chem. Phys. **8**, 1505 (2006).
[26] B. K. Coppa, C. C. Fulton, P. J. Hartlieb, R. F. Davis, B. J. Rodriguez, B. J. Shields, and R. J. Nemanich, J. Appl. Phys. **95**, 5856 (2004).
[27] S. Tanuma, C. J. Powell, and D. R. Penn, Surf. Interface Anal. **35**, 268 (2003).
[28] L. V. Koplitz, O. Dulub, and U. Diebold, J. Phys. Chem. B **107**, 10583 (2003).
[29] M. Kroll and U. Köhler, Surf. Sci. **601**, 2182 (2007).